

Modeling Reservation-Based Autonomous Intersection Control in VISSIM

Zhixia Li, Madhav V. Chitturi, Dongxi Zheng, Andrea R. Bill,
and David A. Noyce

The use of autonomous vehicles is attracting more and more attention as a promising approach to improving both highway safety and efficiency. Most previous studies on autonomous intersection management relied heavily on custom-built simulation tools to implement and evaluate their control algorithms, but the use of nonstandard simulation platforms makes the comparison of systems almost impossible. Furthermore, without support from standard simulation platforms, reliable and trustworthy simulation results are hard to obtain. In this context, this paper explores a way to model autonomous intersections through the use of VISSIM, a standard microscopic simulation platform. A reservation-based intersection control system named autonomous control of urban traffic (ACUTA) was introduced and implemented in VISSIM through the use of VISSIM's external driver model. The operational and safety performance characteristics of ACUTA were evaluated with VISSIM's easy-to-use evaluation tools. In comparison with the results obtained with optimized signalized control, significantly reduced delays, along with a higher intersection capacity and lower volume-to-capacity ratios under various traffic demand conditions, resulted from the use of ACUTA. The safety performance of ACUTA was evaluated by use of the surrogate safety measure model, and few conflicts between vehicles within the intersection were detected. Moreover, the key steps and elements for implementation of ACUTA in VISSIM were introduced. These steps and elements can be useful for other researchers and practitioners implementing their autonomous intersection control algorithms in a standard simulation platform. By use of a standard simulation platform, the performance characteristics of autonomous intersection control algorithms can eventually be compared.

With the rapid advances in sensing, information processing, machine learning, control theory, and automotive technology, the widespread application of autonomous vehicles on highway systems is no longer a dream but will be a reality in the near future. Autonomous vehicles are vehicles that operate without human intervention (in-vehicle or remote) and are capable of driving in real-world highway systems by performing complex tasks such as merging, weaving, and driving through intersections. Many automotive manufacturers, including General Motors, Ford, Mercedes-Benz, Volkswagen, Audi, BMW,

Volvo, and Cadillac, have already begun testing their autonomous vehicles on highway systems (1). Google is also developing and testing its Google driverless car. As of 2012, Florida, Hawaii, Nevada, Oklahoma, and California have legalized or are considering legalization of autonomous cars (1). All these facts indicate that autonomous vehicles are set to appear on roads in the near future.

Most field tests for autonomous vehicles have been restricted to highway segments. Researchers have studied the control of autonomous vehicles at intersections (2–19); however, implementation in practice is difficult because intersections create more conflict points than highway segments. For example, when vehicles arrive at an intersection from different approaches, the right-of-way for traversal of the intersection needs to be determined. Traditional intersections use traffic control devices, such as stop signs and traffic signals, to regulate the rights-of-way of vehicles. For management of autonomous vehicles at intersections, the right-of-way may be controlled by an intersection central controller through vehicle-to-infrastructure communications (2–12) or through negotiation between vehicles via vehicle-to-vehicle communications (13–17).

Studies have been conducted to explore ideas and algorithms for the management of autonomous vehicles at intersections. By the control strategy used, the autonomous intersection control can be classified into centralized control and decentralized control. For centralized control, all vehicles establish communication connections to an intersection central controller or intersection manager (IM) (2–12). The IM determines the passing sequence for the vehicles. Decentralized control systems do not have an IM. The passing sequence is typically negotiated by the vehicles on the basis of a certain protocol (13–17). Among all these available solutions, the reservation-based centralized control system has been found to work the best for urban intersections with high traffic demand because of its mechanism of maximizing intersection capacity (14).

Because of the complexity of field implementation, most researchers used traffic simulation to validate the strategies that they developed for autonomous intersection control. However, none of the existing studies used standard commercial traffic simulation software, such as VISSIM or CORSIM, when evaluating the performance of their proposed strategies. Rather, simulation tools developed by the respective authors were used in the evaluation process, but the use of custom-built simulation tools made the results less reliable and made it hard to compare the results of various studies with each other. In addition, it was noticed that most existing studies lacked standard usage for terms and clear descriptions of simulation parameter settings when presenting the evaluation results. For example, when the traffic volumes were presented, no clarification of whether the volume was per lane or per entire approach was presented. Terms to define lane configurations, speed distribution, volume, and delay, as well

Z. Li and D. Zheng, Room 1249A; M. V. Chitturi and A. R. Bill, Room B243; and D. A. Noyce, Room 1204, Traffic Operations and Safety Laboratory, Department of Civil and Environmental Engineering, Engineering Hall, 1415 Engineering Drive, University of Wisconsin–Madison, Madison, WI 53706. Corresponding author: Z. Li, zli262@wisc.edu.

Transportation Research Record: Journal of the Transportation Research Board, No. 2381, Transportation Research Board of the National Academies, Washington, D.C., 2013, pp. 81–90.
DOI: 10.3141/2381-10

as the number of runs per experiment, random seed selection, and simulation period, were also excluded from the analyses or were not consistently defined across different studies. The inconsistency is most likely due to the use of different custom-built simulation software programs rather than standard commercial simulation software packages.

Standard simulation packages like VISSIM and CORSIM can provide standard parameter settings and outputs. In addition, use of a standard package can guarantee reliable modeling of vehicle generation, car following, lane changing, and many other driving behaviors in the simulation. Flexible settings for speed distribution, percentage of heavy vehicles, and the distributions of acceleration and deceleration rates can also be achieved simply, along with strong evaluation outputs, such as travel time and delay. Moreover, commercial packages like VISSIM have options to output vehicle trajectories, which can be directly imported into the surrogate safety assessment model (SSAM) to analyze the safety performance of the intersection (19).

Wu et al. indicated that they developed their own simulation tool rather than use standard traffic simulation packages, such as VISSIM, AIMSUN, or PARAMICS, because the standard packages do not allow vehicles to be controlled individually (14). In fact, VISSIM offers flexible customization functions to facilitate the building of different special applications through application programming interfaces and component object model (COM) extensions. All these functions offer the potential to implement applications for autonomous intersection control. In this paper, implementation of a reservation-based system in VISSIM with VISSIM's external driver model (EDM) is presented. The establishment of the simulation model, implementation of the reservation-based control algorithm, and finally, evaluations of operational and safety performance are discussed.

ENHANCED RESERVATION-BASED AUTONOMOUS INTERSECTION CONTROL

A reservation-based system uses a centralized control strategy for managing fully autonomous vehicles at an intersection. All vehicles in a reservation-based system communicate only with a centralized intersection controller, namely, the IM. The IM regulates the intersection by determining the passing sequence of all the approaching vehicles (2–10).

The system presented in this paper is named the autonomous control of urban traffic (ACUTA), which is developed on the basis of a first-

come-first-served reservation-based protocol (2) with enhancements to improve some operational issues identified in previous studies (2, 8). These issues include starvation, in which approaching vehicles on the side street cannot get reservations when the traffic demands on the major and side streets are unbalanced, and slow-speed reservation, which unnecessarily occupies many intersection resources. ACUTA regulates an intersection that is divided into a mesh of *n*-by-*n* tiles, as shown in Figure 1, where *n* is termed granularity and reflects the tile density of the intersection mesh.

In ACUTA, each approaching vehicle sets up a communication connection with the IM after it enters the IM's communication range. When it is connected, the vehicle immediately sends the IM a reservation request, along with the vehicle's location, speed, and routing information (i.e., whether it will be making a left or right turn or going straight), indicating its intention to traverse the intersection. The IM processes the reservation request by computing the time-spaces (i.e., intersection tiles that will be occupied by the requesting vehicle for all simulation steps when the vehicle traverses the intersection) required for the vehicle to get through the intersection on the basis of the location, speed, maximum acceleration rate, and routing information provided by the requesting vehicle. Acceleration from the requesting vehicle's current location to the entrance boundary of the intersection is considered when the required time-spaces are computed. The use of different acceleration rates can significantly change the required time-spaces. The alternative acceleration rate will fall within the range from 0 to the maximum acceleration rate of the particular vehicle and is calculated by the following equation:

$$a_i = 0 \quad (i = 1)$$

$$a_i = a_{max} - (i - 1) \frac{1}{m} a_{max} \quad (i > 1) \tag{1}$$

where

- a_i = *i*th alternative acceleration rate (ft/s²),
- a_{max} = maximum acceleration rate (ft/s²), and
- m = maximum number of internal simulations.

The maximum acceleration rate is one of the characteristics particularly pertaining to the requesting vehicle. However, the vehicle must maintain a constant speed when traversing the intersection. In other words, after the vehicle's center point enters the intersection, the vehicle's speed does not change until the vehicle completely clears the intersection. The IM checks whether the required inter-

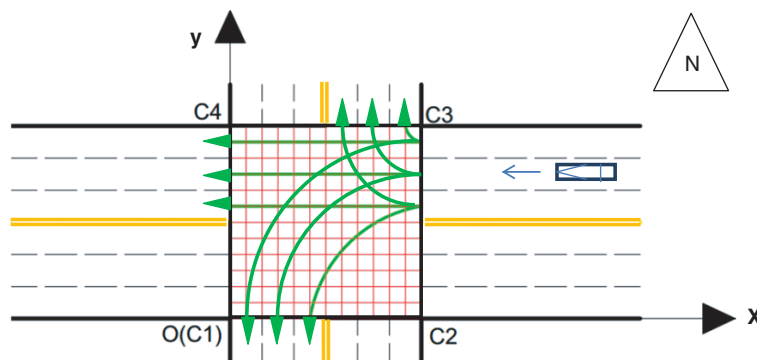


FIGURE 1 Intersection mesh of tiles and example of vehicle's possible routing decisions (O = origin; C1 = southwest corner; C2 = southeast corner; C3 = northeast corner; C4 = northwest corner).

section tiles have already been reserved by other vehicles at every simulation step. If a conflict is detected, an alternative acceleration rate will be used to compute the required time–spaces, and conflicts will again be checked on the basis of the updated required time–spaces. This iterative process is called “internal simulation.” The maximum number of trials of the alternative acceleration rates is termed the “maximum number of internal simulations.” If all alternative acceleration rates are tried out in the internal simulation and conflicts in reservation still exist, the reservation request will be rejected; otherwise, the reservation request will be approved by the IM. The IM automatically rejects the requests from a vehicle following a vehicle that has no reservation.

After a decision is made to reject a reservation request, the IM sends a rejection message to the requesting vehicle with a designated deceleration rate, which can be calculated by the following equation:

$$a_{\text{dec}} = \frac{v_0^2}{2(s_0 - d_0 - v_0\delta)} \quad (2)$$

where

- a_{dec} = designated deceleration rate (ft/s²),
- v_0 = vehicle speed at time that it submitted request (ft/s),
- s_0 = vehicle distance from intersection at time that it submitted request (ft),
- δ = vehicle response time (s), and
- d_0 = distance from intersection to advance stop location (ft).

The vehicle response time (δ) in Equation 2 is the time interval between the instant that a vehicle receives a rejection message from the IM and the instant that the vehicle applies the deceleration rate. The variable δ is analogous to the driver’s perception–reaction time in vehicles operated by humans. In ACUTA, the default value of δ is 0, which assumes ideal conditions with a negligible response time. This assumption is based on the research finding that dedicated short-range communications, which are widely used in connected vehicles research, can achieve negligible delays in milliseconds for the transmission of messages and activation of in-vehicle safety applications (20, 21). For the simplicity of modeling, the millisecond delay is assumed to be 0 in the current version of ACUTA.

The advance stop location (d_0) in Equation 2 is a special parameter in ACUTA that designates a predefined advance stop location other than the traditional stop line close to the intersection for vehicles with rejected reservations. The advance stop location is introduced in ACUTA as a major enhancement strategy to address the slow-reservation-speed issue pertaining to vehicles stopping at the traditional stop line. By use of the advance stop location, vehicles with rejected reservations can stop at a location upstream from the entrance to the intersection and therefore gain a higher speed when they reach the entrance point to the intersection. A higher entrance speed can increase the chance that the vehicle will get a reservation and, meanwhile, save intersection time–space resources through a reduction in the vehicle’s total traversal time within the intersection. A vehicle with a rejected reservation request will apply the designated deceleration rate and start to decelerate as soon as the rejection message is received. The vehicle keeps sending reservation requests until the request is finally approved by the IM.

If the IM approves a reservation request, it sends an approval message to the requesting vehicle along with a designated acceleration rate that will result in no conflicts with existing reservations.

Time stamps indicating when to end the acceleration and when to completely clear the intersection are also sent to the vehicle in the approval message. The approved vehicle will follow the acceleration instruction as soon as it receives the approval message and until it completely clears the intersection.

MODELING OF ACUTA IN VISSIM

Implementation of ACUTA in VISSIM is realized in this research. This section presents the method in which the ACUTA algorithm is modeled in VISSIM. Establishment of the simulation model, the algorithm for determining occupied intersection tiles, and implementation of ACUTA with the VISSIM EDM are elaborated.

Simulation Model of ACUTA Intersection

ACUTA was modeled at a four-legged intersection with three lanes per direction, as shown in Figure 2a. Unlike vehicles at traditional signalized intersections, vehicles can turn from any lane in an ACUTA intersection (Figure 2b) to eliminate the en route lane changes required for turning vehicles. Lane changes are a significant factor contributing to vehicle delays because of conflicts caused by vehicle lane change maneuvers. Each lane in the simulation model was built as a separate link to simplify the simulation model.

Each approach to the intersection is more than 2,000 ft long with a fixed lane width of 12 ft. The input traffic volume of each lane is identical to create balanced traffic demands from all lanes of the intersection. Each lane has three routing decisions: left turn, through, and right turn. The volumes assigned to the routing decisions are the same for all lanes, namely, 25% for left turn, 60% for through, and 15% for right turn. Figure 2c illustrates the routing decisions of a particular lane. The vehicle composition used is 93% passenger cars and 7% heavy vehicles. The speed distribution of traffic is also fixed at a setting equivalent to the 30-mph speed limit. These settings of VISSIM parameters, such as approach length, volume distribution, and heavy vehicle percentage, made it a unique case of simulation. VISSIM provides simple options to change its parameter configurations, including all of the aforementioned settings. Different settings are not expected to make ACUTA more complicated.

No priority rules, conflict areas, desired speed decisions, areas of reduced speed, traffic signals, or stop signs are used in the simulation model, because the traffic control at the intersection is governed only by the IM. Figure 2d provides a screenshot of a simulation run, in which the black vehicles are vehicles that do not have a reservation, gray vehicles are vehicles that have a reservation and that are in the process of passing the intersection, and white vehicles are those that have already cleared the intersection.

Implementation of ACUTA with Use of VISSIM’s EDM

Before the VISSIM EDM was selected for use in the implementation of ACUTA, the feasibility of the use of the VISSIM COM interface and the VISSIM C2X application programming interface was investigated. The C2X application programming interface specializes in modeling of car–car communications with a designated communication range for each vehicle. Therefore, by use of the C2X application programming interface, it might not be possible to obtain information from all of the vehicles, which is not appropriate for implementation of a centralized control strategy. The COM interface

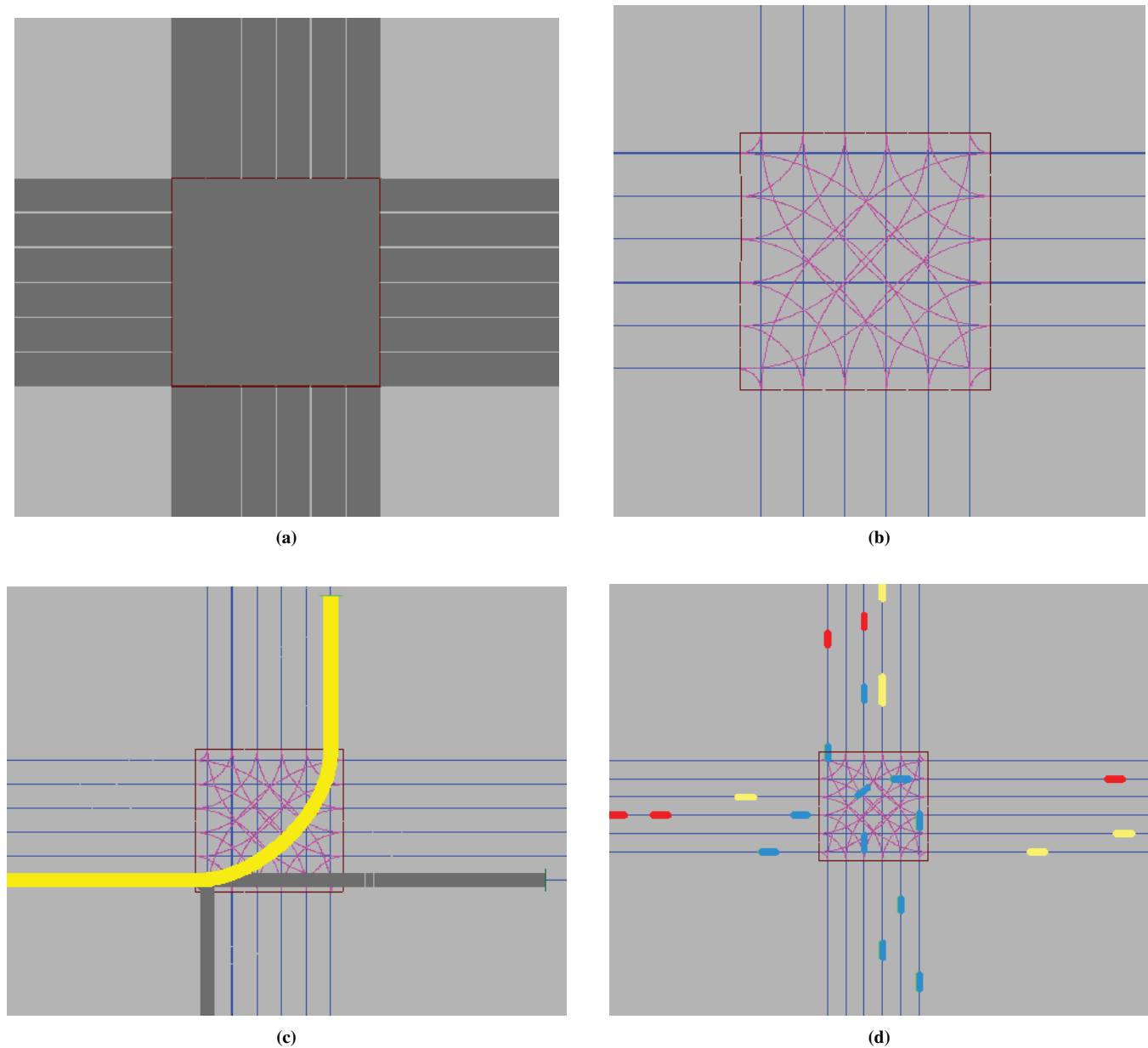


FIGURE 2 Simulation model of ACUTA intersection.

is quite flexible and versatile in collecting vehicle information and modifying vehicle parameters during the simulation period. However, the COM interface does not provide a direct function to modify a vehicle's acceleration rate. It was also found that execution of a command through the COM interface may take up to 0.2 s, which is too long to ensure the efficiency of ACUTA simulations.

The VISSIM EDM, however, can meet all requirements for the implementation of ACUTA. Through EDM, VISSIM provides an option to bypass and replace VISSIM's internal driving behavior. During a simulation run, VISSIM calls the EDM dynamic link library at every simulation step to pass the current state of each vehicle to the dynamic link library. Therefore, in this research, an IM class was built in the EDM dynamic link library to collect each vehicle's speed, location, vehicle class, maximum acceleration rate, length, width, and many other parameters pertaining to the particular vehicle at each

simulation step. The IM processes all reservation requests at the beginning of each simulation step and passes its decision and the suggested acceleration or deceleration rate to the vehicles in the same simulation step. The vehicle then passes its acceleration or deceleration rate back to VISSIM at the same simulation step; thus, the real-time control of each vehicle's acceleration rate is realized.

In summary, EDM offers technical readiness for the implementation of ACUTA in VISSIM. Key steps for realization of the reservation-based system are discussed in the following subsections.

Modeling of Intersection Mesh in VISSIM

In VISSIM, an intersection can be viewed as an overlapping square between the two crossing roads. The entire intersection area can

be divided into a mesh of n -by- n tiles, as shown in Figure 1. n is the granularity of the intersection mesh. More or fewer tiles can be obtained by adjustment of the granularity. By use of the westbound direction as an example, the green lines with arrows in Figure 1 illustrate all possible vehicle paths for traversal of the intersection.

In Figure 1, a two-dimensional coordinate system is projected onto the intersection area to facilitate the computation of a vehicle's location. The origin O is located at the southwest corner (C1) of the intersection. The following sections use this coordinate system as a global coordinate system to compute a vehicle's location.

Locating Vehicle's Central Point

A key step in the internal simulation is to compute a vehicle's location at a given simulation time step. For convenience in the following discussion, the time that represents the beginning is assumed to be the moment when a vehicle's central point reaches the boundary of the intersection area (i.e., point S in Figure 3).

In ACUTA, a vehicle maintains a constant speed after its central point [identified by the coordinates (location) $D(x_t, y_t)$ in Figure 3] enters and before its central point clears the intersection area. Figure 3a illustrates a case of through movement. The path of a through vehicle is parallel to either of the axes (Figure 3a), depending on whether the vehicle is going eastbound or westbound or whether it is going northbound or southbound. If it is assumed that the through vehicle's central point reaches the boundary point $S(x_s, y_s)$ at time zero, the coordinates of the vehicle's central point can be calculated by the following equation:

$$\begin{cases} x_t = x_s - L \\ y_t = y_s \end{cases} \quad (3)$$

where

- x_t = x -coordinate of vehicle's central point at time t (ft),
- y_t = y -coordinate of vehicle's central point at time t (ft),
- x_s = x -coordinate of vehicle's central point at time zero (ft),
- y_s = y -coordinate of vehicle's central point at time zero (ft), and
- $L = v \times t$ (ft), where v is speed of vehicle (ft/s) when it is in intersection and t is any time (s) when vehicle's central point is within intersection.

For turning movements, the vehicle's path within the intersection can be modeled as arcs whose center coordinates are known (the left turn shown in Figure 3b and the right turn shown in Figure 3c, with the arc centers denoted P). If it is assumed that the left-turning vehicle's central point reaches the boundary point $S(x_s, y_s)$ at time zero, the coordinates of the vehicle's central point can be calculated by the following equation:

$$\begin{cases} x_t = x_p - R \times \sin(\alpha + \beta) \\ y_t = y_p + R \times \cos(\alpha + \beta) \end{cases} \quad (4)$$

where

- x_p = x -coordinate of turning arc's center (ft);
- y_p = y -coordinate of turning arc's center (ft);

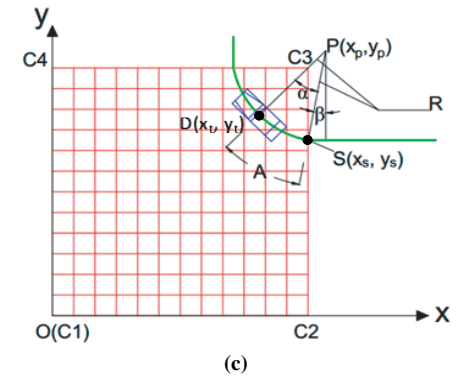
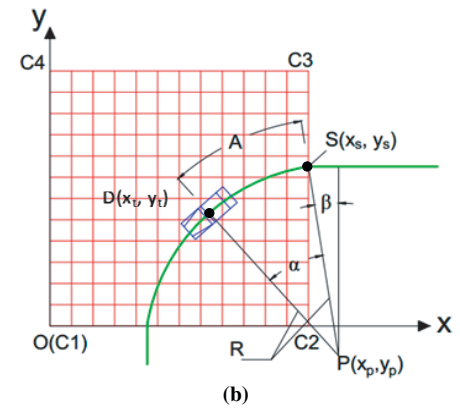
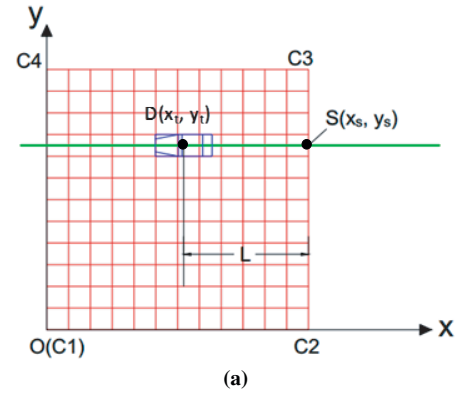


FIGURE 3 Determination of vehicle central point location in intersection: (a) through movement, (b) left turn, and (c) right turn.

$R = \sqrt{(x_p - x_s)^2 + (y_p - y_s)^2}$, which is the radius of the turning arc (ft);
 $\alpha = A/R$ (radians), where A is the arc length (ft), or $v \times t$; and
 $\beta = \arctan(|x_p - x_s|/|y_p - y_s|)$ (radians).

Similarly, if it is assumed that the right-turning vehicle's central point reaches the boundary point $S(x_s, y_s)$ at time zero, the coordinates of the vehicle's central point can be calculated by the following equation:

$$\begin{cases} x_t = x_p - R \times \sin(\alpha + \beta) \\ y_t = y_p - R \times \cos(\alpha + \beta) \end{cases} \quad (5)$$

Calculating Coordinates of Vehicle Vertices

Representation of a vehicle with its central point is not adequate to describe a vehicle's location. A more comprehensive representation of a vehicle is the coordinates of the vehicle's vertices. Figure 4 illustrates the vehicle's vertices in the intersection mesh. In Figure 4, the length of the rectangle is l_v , and the width of the rectangle is w_v , which are equal to the corresponding vehicle's length and width, respectively. The vertices of the rectangle represent the four corners of a vehicle: head left (PT_{HL}), head right (PT_{HR}), tail left (PT_{TL}), and tail right (PT_{TR}). When the coordinates of the vehicle's central point are known, they can be used to calculate the coordinates of the four vertices. When the vehicle is parallel to either of the axes, the coordinates of the four vertices can easily be calculated by use of the central point coordinates by subtraction or addition of an offset of $l_v/2$ or $w_v/2$. When a vehicle is in the position shown in Figure 4, more complex coordinate transformation is needed.

To conduct the coordinate transformation, a local coordinate system (in comparison with the global coordinate system defined in Figure 1) needs to be defined. The origin of the local coordinate system is located at the central point of the vehicle, with the x -axis pointing against the vehicle's traveling direction. To avoid confusion with the global coordinate system, an apostrophe is added to the notations of local coordinate systems (e.g., x' and y' in Figure 4).

Given point (x', y') in the local coordinate system, its coordinates in the global system (x, y) can be calculated by use of a coordinate rotation followed by a coordinate transfer. The formula is given below:

$$\begin{bmatrix} x \\ y \end{bmatrix} = \begin{bmatrix} \cos \theta & -\sin \theta \\ \sin \theta & \cos \theta \end{bmatrix} \times \begin{bmatrix} x' \\ y' \end{bmatrix} + \begin{bmatrix} x_s \\ y_s \end{bmatrix} \quad (6)$$

where θ is the smallest angle measured counterclockwise from the x -axis to the x' -axis. In the case of Figure 1, θ is equal to $\alpha + \beta$ (radians).

On the basis of Equation 6, the global coordinates of the vehicle vertices can easily be converted from their local coordinates. For example, the local coordinates of the PT_{HR} vertex are $(x' = -l_v/2, y' = w_v/2)$. By replacement of x' and y' with $-l_v/2$ and $w_v/2$ in Equation 6, the global coordinates of PT_{HR} are $[x = (-l_v \cdot \cos \theta + w_v \cdot \sin \theta)/2 + x_s, y = (-l_v \cdot \sin \theta - w_v \cdot \cos \theta)/2 + y_s]$.

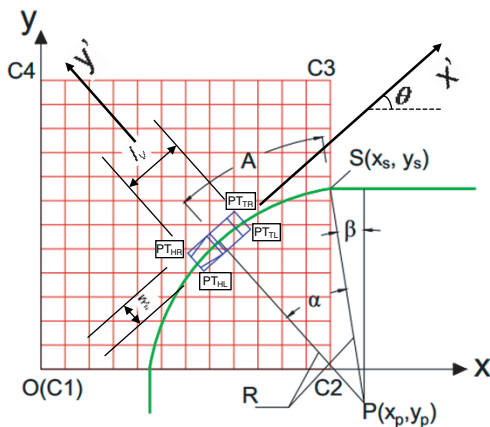


FIGURE 4 Determination of coordinates of vehicle vertices.

Determining Tile Occupation

When the coordinates of a vehicle's vertices are known, the IM needs to determine which tiles are occupied by the vehicle. Figure 5 depicts a vehicle occupying all tiles highlighted in red. The criterion used to determine whether a tile is occupied by a vehicle is as follows: at least one vertex of the tile is inside the vehicle rectangle.

In ACUTA, a vector-based method is used to decide whether a point falls in the vehicle rectangle. As shown in Figure 5, four vectors are defined counterclockwise along the vehicle rectangle. The four vectors are \vec{v}_1 (PT_{HR} → PT_{HL}), \vec{v}_2 (PT_{HL} → PT_{TL}), \vec{v}_3 (PT_{TL} → PT_{TR}), and \vec{v}_4 (PT_{TR} → PT_{HR}). A point is within the vehicle rectangle only if it falls to the left of all four vectors. Given point $p(x_0, y_0)$ and vector $\vec{v}_i [(x_{start}, y_{start}) \rightarrow (x_{end}, y_{end})]$, p falls to the left of \vec{v}_i only when the following formula is satisfied:

$$(x_0 - x_{start}) \times (y_{end} - y_0) - (x_{end} - x_0) \times (y_0 - y_{start}) < 0 \quad (7)$$

where

- x_0 = x -coordinate of testing point (ft),
- y_0 = y -coordinate of testing point (ft),
- x_{start} = x -coordinate of vector's start point (ft),
- y_{start} = y -coordinate of vector's start point (ft),
- x_{end} = x -coordinate of vector's end point (ft), and
- y_{end} = y -coordinate of vector's end point (ft).

However, it is relatively easy to decide whether a vertex of a vehicle rectangle falls in a tile. The reason is that a tile is bounded by two horizontal lines and two vertical lines. More specifically, any point within the area of a tile can be formulated as follows:

$$\begin{cases} x_{low} < x_0 < x_{high} \\ y_{low} < y_0 < y_{high} \end{cases} \quad (8)$$

where

- x_{low} = shared x -coordinate of left vertices of tile (ft),
- y_{low} = shared y -coordinate of bottom vertices of tile (ft),

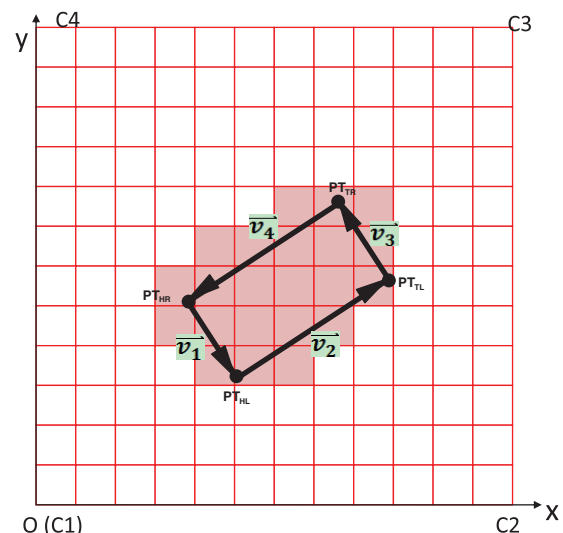


FIGURE 5 Tile occupation by vehicle rectangle.

x_{high} = shared x -coordinate of right vertices of tile (ft), and
 y_{high} = shared y -coordinate of top vertices of tile (ft).

In summary, given a tile and a vehicle rectangle, Equations 7 and 8 are used to judge whether a vehicle rectangle has occupied a tile. If any of the four vertices of a tile satisfies Equation 7 or if any of the four vertices of a vehicle rectangle satisfies Equation 8, the tile is considered occupied by the vehicle.

EVALUATION OF ACUTA PERFORMANCE

VISSIM provides a wide range of evaluation tools for its simulation models. This section discusses the evaluation of ACUTA’s operational and safety performance by use of VISSIM’s evaluation functions.

Operational Performance

ACUTA’s operational performance under different traffic demand conditions was evaluated with the simulation results and was further compared with the performance of a comparable signalized intersection. The signalized intersection modeled in VISSIM has a left-turn lane, a through lane, and a shared through and right-turn lane designated for each approach. Traffic demands for each movement were identical between the ACUTA and the signalized intersection models. All other parameters except lane configurations are identical between the two models.

For each traffic demand condition, five simulation runs with different random seeds were performed. Each simulation run lasted 2,100 s, with the first 300 s of warm-up being dropped from the evaluation. Specifically, the demand for each approach increased from 150 to 2,850 vehicles per hour (veh/h) to cover the possible range of traffic demands. The proportions of traffic demand for left-turn,

through, and right-turn movements were fixed at 25%, 60%, and 15%, respectively, for all simulation runs. Specific demands by movement are summarized in Table 1. For the signalized intersection model, signal timing was optimized through the use of Highway Capacity Software (22). Optimization was conducted for each traffic demand tested. Table 1 lists the phasing and optimized timings for the signalized intersection along with the corresponding optimized cycle lengths.

The operational performance characteristics of ACUTA and optimized signal control were assessed by delays, which were obtained directly from VISSIM’s output. Volume-to-capacity (v/c) ratios for left turn, right turn, and through movements as well as the overall intersection v/c ratio were also computed for both ACUTA and optimized signal control. When v/c ratios were computed, capacity was measured as the maximum throughput among all demand conditions and volume was directly obtained from VISSIM’s output for that specific demand condition.

On the basis of the simulation results, the capacities for the left-turn, right-turn, and through movements at the signalized intersection were identified to be 366, 218, and 908 veh/h, respectively. The capacity for an entire approach of the signalized intersection was 1,480 veh/h. The capacities for left-turn, right-turn, and through movements of an approach at an ACUTA intersection were measured to be 501, 288, and 1,185 veh/h, respectively. The capacity for an entire approach of an ACUTA intersection was 1,974 veh/h. Comparison of ACUTA with signalized control showed that ACUTA successfully increased left-turn, right-turn, and through movement capacities by 37%, 32%, and 31%, respectively. The overall capacity for an approach was increased by 33% by the implementation of ACUTA.

All evaluation results, including the v/c ratios and delays, are summarized in Table 2. The signalized intersection reached an overall v/c ratio of 0.99 when the approach traffic demand was about 1,650 veh/h; ACUTA did not reach an overall v/c ratio of 0.99 until

TABLE 1 Traffic Demand Inputs and Optimized Timing Plan

Approach Traffic Demand (vph)	Approach Demand by Movement (vph)			Signal Timing Plan				
				Cycle Length (s)	Phase Timing (s)			
								
150	38	90	23	40	6	6	6	6
300	75	180	45	40	6	6	6	6
600	150	360	90	60	6	16	6	16
900	225	540	135	60	6	16	6	16
1,050	263	630	158	60	6	16	6	16
1,200	300	720	180	90	10	28	9	27
1,350	338	810	203	90	10	28	9	27
1,500	375	900	225	110	12	35	12	35
1,650	413	990	248	110	12	35	12	35
1,800	450	1,080	270	110	12	35	12	35
1,950	488	1,170	293	110	12	35	12	35
2,100	525	1,260	315	110	12	35	12	35
2,400	600	1,440	360	120	12	39	13	40
2,850	713	1,710	428	120	12	39	13	40

NOTE: LT = left turn; RT = right turn.

TABLE 2 Comparison of Operational Performance Characteristics Between ACUTA and an Optimized Signalized Intersection

Approach Traffic Demand (vph)	Optimized Signalized Control								ACUTA (default setting)							
	v/c Ratio				Delay (s/veh)				v/c Ratio				Delay (s/veh)			
	LT	Through	RT	Overall	LT	Through	RT	Overall	LT	Through	RT	Overall	LT	Through	RT	Overall
150	0.10	0.10	0.10	0.10	7.36	15.54	17.06	13.70	0.07	0.07	0.07	0.07	0.00	0.00	0.00	0.00
300	0.22	0.19	0.20	0.20	9.26	15.90	17.26	14.34	0.12	0.12	0.12	0.12	0.00	0.00	0.00	0.00
600	0.45	0.39	0.39	0.40	13.12	17.72	20.74	16.90	0.31	0.28	0.31	0.29	0.00	0.00	0.00	0.00
900	0.65	0.59	0.59	0.61	21.52	19.74	22.48	20.62	0.49	0.43	0.45	0.45	0.04	0.04	0.06	0.02
1,050	0.75	0.69	0.69	0.71	36.24	21.04	24.38	25.48	0.55	0.51	0.53	0.52	0.26	0.42	0.44	0.38
1,200	0.84	0.79	0.79	0.81	53.62	28.70	32.56	35.66	0.62	0.59	0.61	0.60	0.98	0.70	0.76	0.78
1,350	0.90	0.88	0.89	0.89	118.72	35.82	38.68	56.86	0.70	0.67	0.67	0.68	1.46	1.48	1.64	1.50
1,500	0.92	0.96	0.95	0.96	186.70	53.02	56.64	85.44	0.77	0.76	0.74	0.76	2.82	2.30	2.14	2.42
1,650	0.97	0.98	0.99	0.99	230.04	81.46	84.82	117.90	0.84	0.83	0.83	0.83	5.16	4.98	4.32	4.94
1,800	0.98	0.98	0.98	0.99	278.72	133.74	137.08	169.42	0.90	0.90	0.87	0.89	25.70	24.78	24.12	24.90
1,950	0.98	0.99	0.98	0.99	298.04	161.54	162.30	194.98	0.91	0.91	0.89	0.91	97.00	100.20	97.86	99.04
2,100	0.97	1.00	1.00	1.00	331.78	182.34	184.22	218.32	0.99	0.99	0.98	0.99	102.20	104.04	102.52	103.34
2,400	0.99	0.98	0.98	0.99	336.26	206.02	204.48	237.88	0.97	0.96	0.96	0.96	198.72	205.50	200.64	203.06
2,850	1.00	0.98	0.98	0.99	355.66	211.78	213.28	247.86	1.00	1.00	1.00	1.00	227.24	231.28	226.52	229.58

NOTE: s/veh = number of seconds per vehicle.

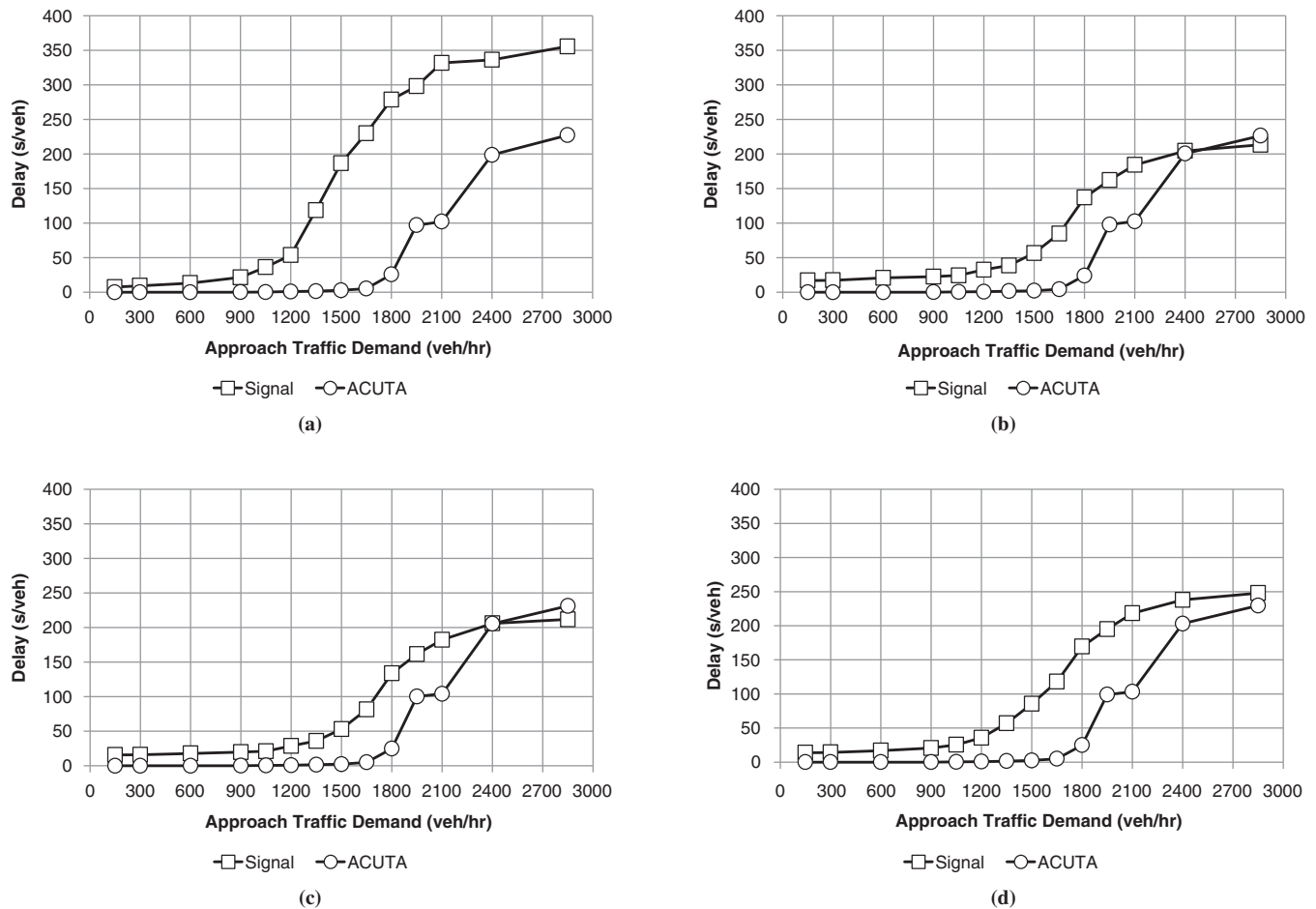


FIGURE 6 Operational performance of ACUTA by comparison with signalized intersection: (a) left-turn delay, (b) right-turn delay, (c) through delay, and (d) overall intersection delay.

the approach traffic demand reached 2,100 veh/h. These facts indicate that the ACUTA intersection can process an additional 450 vehicles per hour per approach compared with the number that the optimized signalized intersection can process without being oversaturated.

Figure 6 depicts the relationships between the delays and traffic demands. Figure 6, *a* through *c*, illustrates the delays for left-turn, right-turn, and through movements, respectively. Figure 6 indicates that the operational performance of different traffic movements in ACUTA was balanced, as the delays for left-turn, right-turn, and through movements were similar under all traffic demand conditions. The overall intersection delay shown in Figure 6*d* was computed from the weighted average of the delays for all movements. According to Figure 6*d*, overall intersection delay for ACUTA remained at an extremely low level (less than 5 s per vehicle) when approach traffic demand was less than 1,650 veh/h, and the signalized intersection already started to operate at near capacity conditions when approach traffic demand reached 1,350 veh/h. The delay for ACUTA started to increase rapidly when traffic demand reached 1,800 veh/h. However, the delays were still significantly less than the delays for the signalized intersection for approach traffic demands of greater than 1,800 veh/h and less than 2,100 veh/h. The superiority of ACUTA became marginal at extremely high approach traffic demands of 2,400 and 2,850 veh/h.

Safety Performance

VISSIM can output vehicle trajectories, which can be directly imported into SSAM to analyze traffic conflicts. This capability enables evaluation of the safety performance of ACUTA. The result of a safety performance study of ACUTA with SSAM is shown in Figure 7, which illustrates an example of a conflict map obtained from SSAM. Only one traffic conflict was found within the intersection during a simulation run of 1,800 simulation seconds. This conflict could have been eliminated by incorporation of a safety buffer, which will be done in the next phase of this study.

CONCLUSIONS

A major contribution of this research is the successful implementation of a reservation-based autonomous intersection system in a standard simulation platform, VISSIM. The feasibility of the use of VISSIM's EDM for modeling of autonomous vehicle operations at a centralized controlled intersection through vehicle-to-infrastructure communications has been demonstrated. This type of implementation has not been realized before or even been discussed in the literature. Key steps for the implementation of ACUTA in VISSIM were introduced

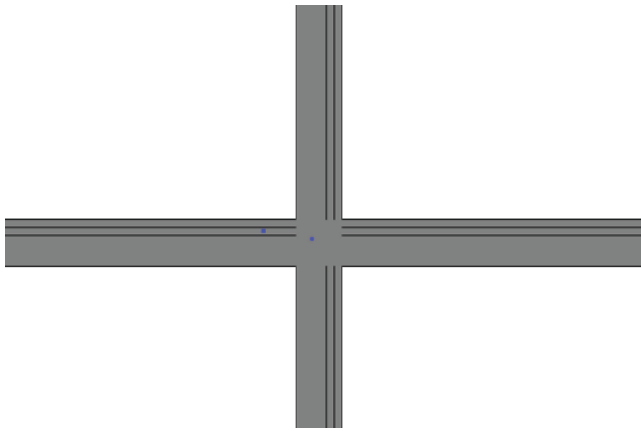


FIGURE 7 Conflict map from SSAM.

in this paper and will serve as a reference to other researchers who are interested in implementing autonomous intersections in a standard simulation platform. By use of a standard simulation platform, simulation results can become more reliable and trustworthy. The most important result is that the operational performance of different autonomous intersection control algorithms will eventually be able to be compared under the same simulation platform.

Evaluation results obtained from VISSIM demonstrated that ACUTA operated with a high efficiency (i.e., intersection delays of <5 s per vehicle) when the approach traffic demand was less than 1,650 veh/h. In addition, ACUTA had balanced delay distributions for left-turn, right-turn, and through movements under all traffic demand conditions. Comparison of ACUTA with optimized signal control showed that ACUTA successfully increased left-turn, right-turn, and through capacities by 37%, 32%, and 31%, respectively. The overall approach capacity was increased by 33% by the implementation of ACUTA. The analysis of the v/c ratios indicated that the ACUTA intersection could process an additional 450 vehicles per hour per approach compared with the number that the optimized signalized intersection could process without being oversaturated. Finally, the safety assessment showed only one conflict during a simulation run. All these findings indicate that ACUTA can be well modeled in the VISSIM environment.

ACKNOWLEDGMENT

The research presented in this paper was funded by the National Center for Freight and Infrastructure Research and Education at the University of Wisconsin–Madison.

REFERENCES

1. Wikipedia. *Autonomous Car*. http://en.wikipedia.org/wiki/Autonomous_car#cite_note-24. Accessed July 31, 2012.
2. Dresner, K., and P. Stone. Multiagent Traffic Management: A Reservation-Based Intersection Control Mechanism. *Proc., Third International Joint Conference on Autonomous Agents and Multiagent Systems*, New York, July 2004, pp. 530–537.
3. Dresner, K., and P. Stone. Multiagent Traffic Management: An Improved Intersection Control Mechanism. *Proc., Fourth International Joint Conference on Autonomous Agents and Multiagent Systems*, Utrecht, Netherlands, July 2005, pp. 471–477.
4. Dresner, K., and P. Stone. Turning the Corner: Improved Intersection Control for Autonomous Vehicles. *Proc., 2005 IEEE Intelligent Vehicles Symposium*, Las Vegas, Nev., June 2005.
5. Dresner, K., and P. Stone. A Multiagent Approach to Autonomous Intersection Management. *Journal of Artificial Intelligence Research*, Vol. 31, 2008, pp. 591–656.
6. Dresner, K., and P. Stone. Mitigating Catastrophic Failure at Intersections of Autonomous Vehicles. *Proc., Seventh International Conference on Autonomous Agents and Multiagent Systems*, Estoril, Portugal, May 2008, pp. 1393–1396.
7. Shahidi, N., T. C. Au, and P. Stone. Batch Reservations in Autonomous Intersection Management. *Proc., 10th International Conference on Autonomous Agents and Multiagent Systems*, Vol. 3, Richland, S.C., 2011.
8. Au, T. C., N. Shahidi, and P. Stone. Enforcing Liveness in Autonomous Traffic Management. *Proc., 25th Association for the Advancement of Artificial Intelligence Conference of Artificial Intelligence*, 2011, pp. 1317–1322.
9. Quinlan, M., T. C. Au, J. Zhu, N. Sturca, and P. Stone. Bringing Simulation to Life: A Mixed Reality Autonomous Intersection. *Proc., 2010 IEEE/Robotics Society of Japan International Conference on Intelligent Robots and Systems*, 2010.
10. Fajardo, D., T.-C. Au, S. T. Waller, P. Stone, and D. Yang. Automated Intersection Control: Performance of Future Innovation Versus Current Traffic Signal Control. In *Transportation Research Record: Journal of the Transportation Research Board*, No. 2259, Transportation Research Board of the National Academies, Washington, D.C., 2011, pp. 223–232.
11. Wu, J., A. Abbas-Turki, and A. El Moudni. Intersection Traffic Control by a Novel Scheduling Model. *Proc., IEEE/INFORMS International Conference on Service Operations, Logistics and Informatics*, 2009.
12. Yan, F., M. Dridi, and A. El Moudni. Autonomous Vehicle Sequencing Algorithm at Isolated Intersections. *Proc., 12th International IEEE Conference on Intelligent Transportation Systems*, St. Louis, Mo., 2009.
13. Wu, J., A. Abbas-Turki, A. Corréia, and A. El Moudni. Discrete Intersection Signal Control. *Proc., IEEE International Conference on Service Operations and Logistics, and Informatics*, 2007.
14. Wu, J., A. Abbas-Turki, and A. El Moudni. Contextualized Traffic Controlling at Isolated Urban Intersection. *Proc., 14th World Multi-Conference on Systemics, Cybernetics and Informatics*, 2010.
15. VanMiddlesworth, M., K. Dresner, and P. Stone. Replacing the Stop Sign: Unmanaged Intersection Control for Autonomous Vehicles. *Proc., Autonomous Agents and Multiagent Systems Workshop on Agents in Traffic and Transportation*, Estoril, Portugal, 2008, pp. 94–101.
16. Alonso, J., V. Milanés, P. Joshué, E. Onieva, C. González, and T. de Pedro. Autonomous Vehicle Control Systems for Safe Crossroads. *Transportation Research Part C*, Vol. 19, No. 6, 2011, pp. 1095–1110.
17. Ball, R., and N. Dulay. Enhancing Traffic Intersection Control with Intelligent Objects. *Proc., First International Workshop in the Urban Internet of Things*, 2010.
18. Vasirani, M., and S. Ossowski. Evaluating Policies for Reservation-Based Intersection Control. *Proc., 14th Portuguese Conference on Artificial Intelligence (EPIA '09)*, Vol. 14, 2009.
19. *Surrogate Safety Assessment Model and Validation*. Final report. FHWA-HRT-08-051. FHWA, U.S. Department of Transportation, 2008.
20. *DSRC: The Future of Safer Driving*. Research and Innovative Technology Administration, U.S. Department of Transportation. <http://www.its.dot.gov/factsheets/pdf/JPO-034%20DSRC%20V5.5%20F.pdf>. Accessed Nov. 14, 2012.
21. Hu, B., and H. Gharavi. Joint Vehicle–Vehicle/Vehicle–Roadside Communication Protocol for Highway Traffic Safety. *International Journal of Vehicular Technology*, 2011. doi:10.1155/2011/718048.
22. *Highway Capacity Software*. McTrans, University of Florida, Gainesville, 2000.

The Vehicle–Highway Automation Committee peer-reviewed this paper.